

Superscaling predictions for NC and CC quasi-elastic neutrino-nucleus scattering

J.E. Amaro*, M.B. Barbaro†, J.A. Caballero** and T.W. Donnelly‡

**Departamento de Física Atomica, Molecular y Nuclear, Universidad de Granada, 18071 Granada, Spain*

†*Dipartimento di Fisica Teorica, University of Turin, and INFN Sezione di Torino, 10125 Turin, Italy.*

***Departamento de Física Atomica, Molecular y Nuclear, Universidad de Sevilla. 41080 Sevilla, Spain*

‡*Center for Theoretical Physics, Laboratory for Nuclear Science and Department of Physics, Massachusetts Institute of Technology, Cambridge, MA 02139, USA*

Abstract. Quasielastic double differential neutrino cross sections can be obtained in a phenomenological model based on the superscaling behavior of electron scattering data. In this talk the superscaling approach (SuSA) is reviewed and its validity is tested in a relativistic shell model. Results including meson exchange currents for the kinematics of the MiniBoone experiment are presented.

Keywords: Neutrino induced nuclear reactions

PACS: 25.30.Pt, 24.10.-i, 25.30.Fj

Analysis of inclusive (e, e') data have demonstrated that at energy transfers below the quasielastic (QE) peak superscaling is fulfilled rather well [1]–[3]. The general procedure consist on dividing the experimental (e, e') cross section by an appropriate single-nucleon cross section to obtain the experimental scaling function $f(\psi)$, which is then plotted as a function of the scaling variable ψ for several kinematics and for several nuclei. If the results do not depend on the momentum transfer q , we say that scaling of the first kind occurs. If there is not dependence on the nuclear species, one has scaling of the second kind. The simultaneous occurrence of scaling of both kinds is called superscaling. The Super-Scaling approach (SuSA) is based on the assumed universality of the scaling function for electromagnetic and weak interactions [4].

The superscaling property is exact in the relativistic Fermi gas model (RFG) by construction, and it has been tested in more realistic models of the (e, e') reaction [5]–[7]. A study of superscaling in the semirelativistic (SR) continuum shell model with Woods-Saxon (WS) mean potential is summarized in Fig. 1. There we show the longitudinal scaling function defined as $f_L = R_L/G_L$, where R_L is the longitudinal response function and G_L is a single-nucleon factor. When $f_L(\psi)$ is plotted for various values of the momentum transfer and for several closed-shell nuclei, all the curves approximately collapse into one. Small violations of scaling are seen at low values of ψ , coming from the low-energy potential resonances for $q = 0.5$ GeV/c, which disappear for higher q values.

While the SR shell model superscales, it does not reproduce the experimental data of the phenomenological scaling function extracted from the longitudinal QE elec-

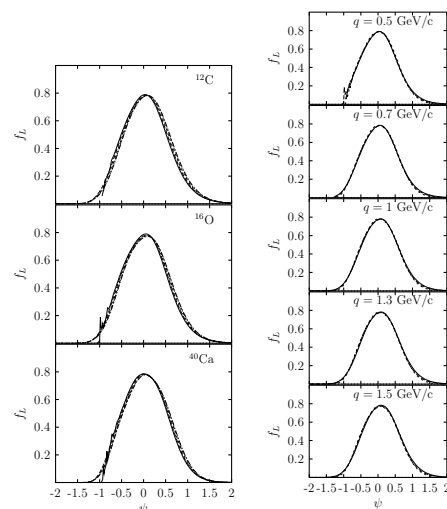


FIGURE 1. Scaling properties of the SR shell model. Left: scaling of the first kind. Curves for $q = 0.5, 0.7, 1, 1.3, 1.5$ GeV collapse into one. Right: scaling of the second kind. Curves for ^{12}C , ^{16}O and ^{40}Ca collapse into one.

tron scattering response. The WS potential used to describe the final-state interaction (FSI) of the ejected proton does not incorporate the appropriate reactions mechanisms. A further improvement of the FSI consist in using the Dirac-Equation based potential plus Darwin term (DEB+D). The DEB potential is obtained from the Dirac equation for the upper component $\psi_{up}(\mathbf{r}) = K(r, E)\phi(\mathbf{r})$, where the Darwin term $K(r, E)$ is chosen in such a way that the function $\phi(r)$ satisfies a Schrödinger-like equation. The electromagnetic L and T scaling functions

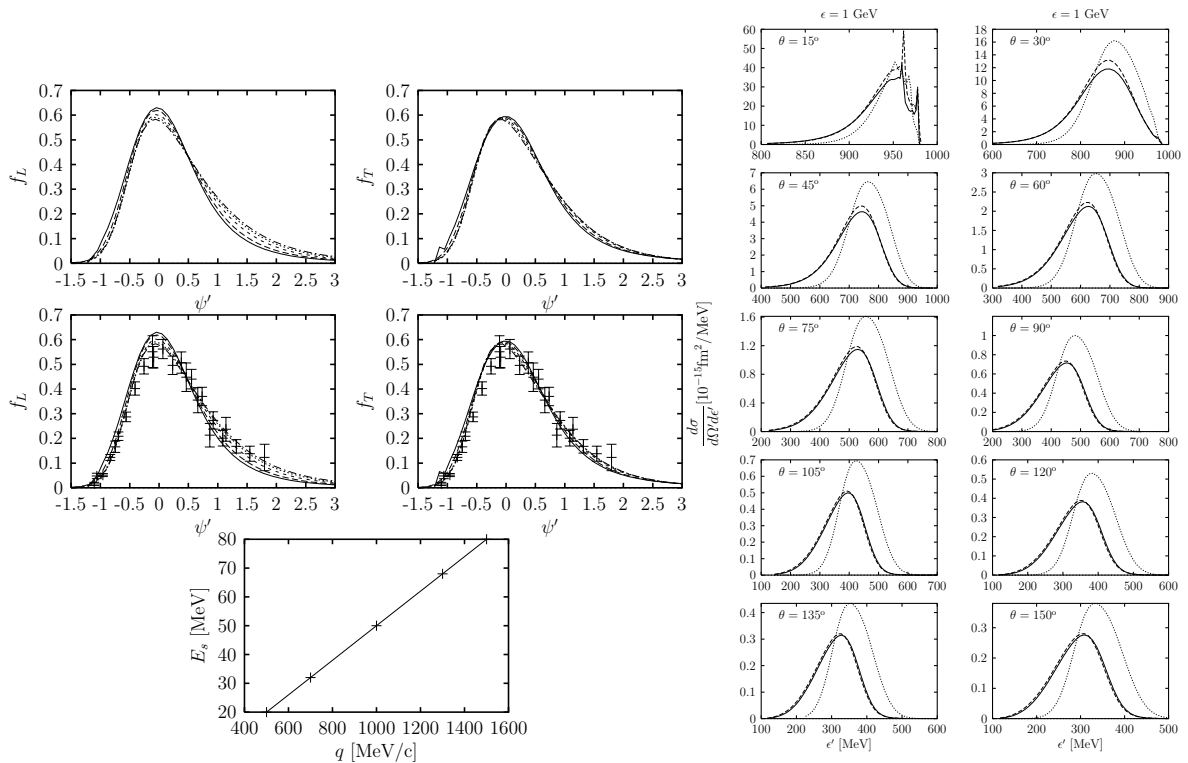


FIGURE 2. Left: Scaling of 1st kind with DEB+D potential compared with experimental data. $q = 0.5, 0.7, 1.0, 1.3$ and 1.5 GeV/c. Right: Test of SuSA in the SR shell model for the $^{12}\text{C}(\nu_\mu, \mu^-)$ reaction with neutrino energy $\varepsilon = 1$ GeV. Dotted: Woods-Saxon potential. Solid: DEB+D potential. Dashed: SuSA reconstruction from the computed (e, e') scaling function.

within this model are shown in Fig. 2. We use the same relativistic Hartree potential as in the relativistic mean field model of [5], and the scaling variable ψ' includes a q -dependent energy shift $E_s(q)$. Although the scaling is not perfect, it is remarkable that our results give essentially the same scaling function for a wide range of q values, reproducing well the phenomenological data.

In Fig. 2 (right) we compare DEB+D and Woods-Saxon predictions for the $^{12}\text{C}(\nu_\mu, \mu^-)$ differential QE cross section for 1 GeV incident neutrinos and for several lepton scattering angles. The SuSA reconstructed cross section is also shown, using the theoretical scaling function extracted from (e, e') results with the DEB+D model (curves in Fig. 2, left). For angles above 15° the SuSA is applicable and its predictions can be considered quite reasonable, with small error.

The superscaling approach has been extended to inclusive neutrino scattering via the weak neutral current [8]. In the (ν, N) reaction a nucleon is detected and the final neutrino must be integrated. We approximate the u -channel inclusive scattering cross section

$$\frac{d\sigma}{d\Omega_N dp_N} \simeq \bar{\sigma}_{sn}^{(u)} F^{(u)}(\psi^{(u)}). \quad (1)$$

In Fig. 3 we see that the above factorization is a good approximation in the RFG, and therefore one could extend

the scaling analysis used for CC reactions to NC scattering. In Fig. 3 we show examples of SuSA predictions of NC cross sections using the phenomenological (e, e') scaling function.

Recently the effect of meson exchange currents (MEC) in (e, e') for high momentum transfer has been investigated [9, 10], and the two-particle emission (2p-2h) diagrams of Fig. 4 have been extended to the CC weak interaction sector [11], in order to explore the role of MEC in neutrino reactions. In Fig. 5 we show that inclusion of 2p-2h contributions yields results for the QE (ν_μ, μ^-) cross section that are comparable with the recent MiniBooNE collaboration data [12] for $\theta \leq 50^\circ$, but lie below the data at larger angles where the predicted cross sections are smaller. The inclusion of the correlation diagrams which are required by gauge invariance [10] plus other relativistic effects might improve the agreement with the data.

This work was partially supported by DGI (Spain): FIS2008-01143, FIS2008-04189, by the Junta de Andalucía, and part (TWD) by U.S. Department of Energy under cooperative agreement DE-FC02-94ER40818.

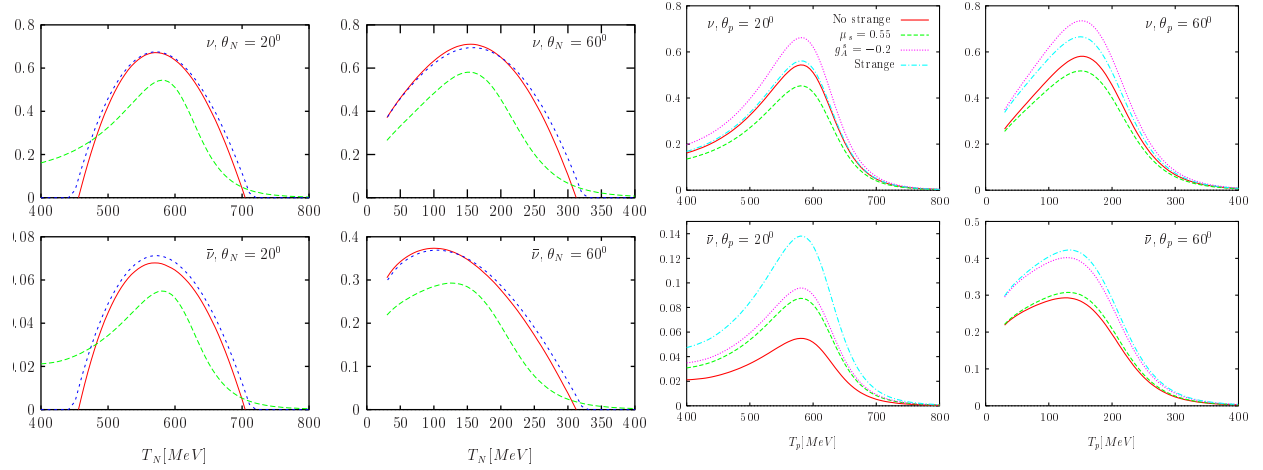


FIGURE 3. Neutral current proton knock-out cross section from ^{12}C . Left: RFG (solid lines), RFG with factorization (dotted lines), and SuSA (dashed lines). Right: study of nucleon strangeness effect.

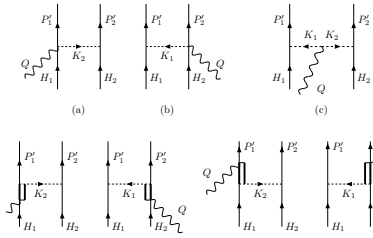


FIGURE 4. Diagrams contributing to the MEC

REFERENCES

1. D.B. Day, J.S. McCarthy, T.W. Donnelly, and I. Sick, *Ann. Rev. Nucl. Part. Sci.* 40, 357 (1990)
2. T.W. Donnelly and I. Sick, *Phys. Rev. Lett.* 82, 3212 (1999).
3. T.W. Donnelly and I. Sick, *Phys. Rev. C* 60, 065502 (1999).
4. J.E. Amaro, M.B. Barbaro, J.A. Caballero, T.W. Donnelly, A. Molinari, I. Sick, *Phys. Rev. C* 71, 015501 (2005).
5. J.A. Caballero, J.E. Amaro, M.B. Barbaro, T.W. Donnelly, C. Maieron, J.M. Udias, *Phys. Rev. Lett.* 95, 252502 (2005).
6. J.E. Amaro, M.B. Barbaro, J.A. Caballero, T.W. Donnelly, and C. Maieron, *Phys. Rev. C* 71, 065501 (2005)
7. J.E. Amaro, M.B. Barbaro, J.A. Caballero, T.W. Donnelly, and J.M. Udias, *Phys. Rev. C* 75, 034613 (2007)
8. J.E. Amaro, M.B. Barbaro, J.A. Caballero, T.W. Donnelly, *Phys. Rev. C* 73, 035503 (2006)
9. J.E. Amaro, M.B. Barbaro, J.A. Caballero, T.W. Donnelly, C. Maieron, J.M. Udias, *Phys. Rev. C* 81, 014606 (2010).
10. J.E. Amaro, C. Maieron, M.B. Barbaro, J.A. Caballero, T.W. Donnelly, *Phys. Rev. C* 82, 044601, (2010)
11. J.E. Amaro, M.B. Barbaro, J.A. Caballero, T.W. Donnelly, C.F. Williamson, *Phys. Lett. B*, to be published. arXiv:1010.1708
12. A.A. Aguilar-Arevalo et al., [MiniBooNE Collaboration], *Phys. Rev. D* 81, 092005 (2010).

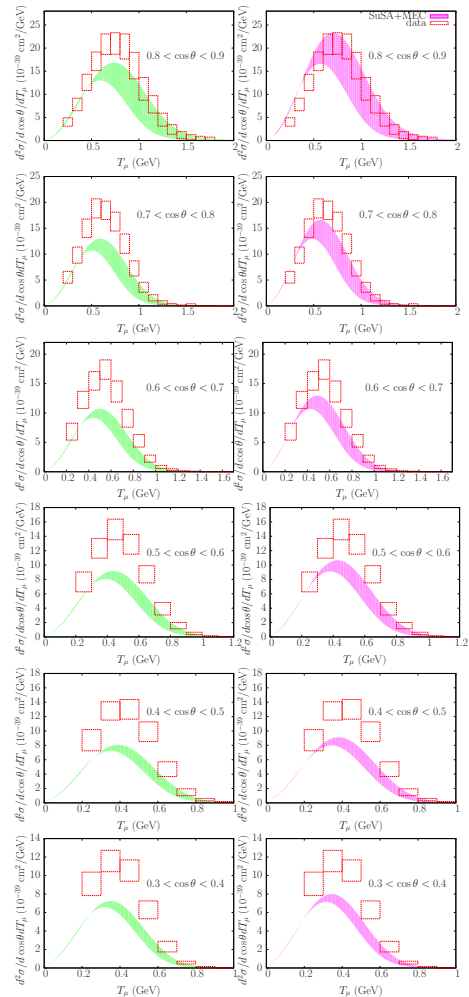


FIGURE 5. Computed QE (ν_μ, μ^-) cross section compared to Miniboone data. Left: SuSA. Right: SuSA + MEC